CHEMISTRY
A EUROPEAN JOURNAL

DOI: 10.1002/chem.200902439

Nanoscale Biomolecular Structures on Self-Assembled Monolayers Generated from Modular Pegylated Disulfides

Lu Shin Wong,[a] Stefan J. Janusz,[b] Shuqing Sun,[b, c] Graham J. Leggett,[b] and Jason Micklefield*[a]

Abstract: A solid-phase synthetic strategy was developed that uses modular building blocks to prepare symmetric oligo(ethylene glycol)-terminated disulfides with a variety of lengths and terminal functionalities. The modular disulfides, composed of alkyl amino groups linked by an amide group to oligoethylene chains were used to generate self-assembled monolayers (SAMs), which were characterised to determine their applicability for biomolecular applications. X-ray photoelectron spectroscopy (XPS) of the SAMs obtained from these molecules demonstrated improved stability towards displacement by 16-hexadecanethiol, while surface plasmon resonance (SPR) analyses of SAMs prepared with the hydroxy-terminated oligoethylene disulfide showed equal resistance to non-specific protein adsorption in comparison to 11-mercaptoundecyl tri(ethylene glycol). SAMs made from these adsorbates were amenable to nanoscale patterning by scanning near-field photolithography (SNP), facilitating the fabrication of nanopatterned, protein-functionalised surfaces. Such SAMs may be further developed for bionanotechnology applications such as the fabrication of nanoscale biological arrays and sensor devices.

Keywords: bionanotechnology · monolayers · photolithography · protein immobilization · self-assembly · solid-phase synthesis

Introduction

Nanofabrication has been exploited in a diverse range of applications from high-sensitivity biomedical diagnostic tools, sensor devices, surface coatings, nanoelectronics, through to single-molecule enzymology and the development of molecular motors.[1–5] Self-assembled monolayers (SAMs) of alkylthiolates on metals have proved to be particularly important platforms for nanotechnology development. Here, SAMs offer a straightforward route to the control of chemistry over macroscopic areas.[6,7] When combined with a lithographic technique,[3,8–14] such as electron beam lithography,[15,16] dip-pen nanolithography[11,17,18] and scanning near-field photolithography (SNP),[14,19,20] patterning of SAMs can be achieved with nanoscale resolution.

SAMs have been widely used as platforms for the study of biological interactions and assembly of biomolecular structures down to the nanoscopic scale. For example, SAMs have been utilised for studies involving enzymatic processing of DNA,[21,22] DNA computing,[23] protein assays[24,25] and studies of cellular responses towards surfaces.[26–28] Following the success of DNA functionalised surfaces in genomic analysis, significant efforts have been made to develop protein and oligosaccharide functionalised chips for proteomics- and glycomics-based research.[29–31] Also, with the ever increasing drive towards smaller sample sizes and higher throughput for whole-organism analysis, has come the need to develop nanometer-scale, biomolecular, patterned surfaces.[3,32,33] However, in order to further exploit SAM-based systems in this context, a number of issues remain to be fully addressed. Firstly, convenient strategies for the synthesis of bespoke thiols (or their equivalents) that are tailored towards specific applications are required.[34] This is especially the case in applications involving patterned surfaces, since several thiol species, one to cover the bulk surface and one or several others at the patterned areas, are required. An additional requirement in biomolecular appli-

[a] Dr. L. S. Wong, Prof. J. Micklefield
School of Chemistry & Manchester Interdisciplinary Biocentre
University of Manchester, 131 Princess Street
Manchester M1 7DN (UK)
Fax: (+44) 161 306 5199
E-mail: j.micklefield@manchester.ac.uk

[b] Dr. S. J. Janusz, Dr. S. Sun, Prof. G. J. Leggett
Department of Chemistry, University of Sheffield
Brook Hill, Sheffield S3 7HF (UK)

[c] Dr. S. Sun
National Centerfor Nanoscience and Technology,
Beijing 100190 (China)

Supporting information for this article is available on the WWW under http://dx.doi.org/10.1002/chem.200902439.

cations is the need to control non-specific adsorption of biomolecules, particularly for proteins for which adsorption can rapidly become irreversible. In this respect, thiols bearing polyethylene glycol (PEG) moieties have emerged as the most widely used materials for the fabrication of such bioresistant SAMs.[7,24,25,35–37] However, these thiols are usually prepared by time-consuming, linear, multistep syntheses, which are inconvenient for the generation of a range of chain lengths and the introduction of further chemical diversity.

In this report, the use of a solid-phase synthesis for the preparation of "pegylated" disulfides, containing oligomeric ethylene glycol units, is explored. The SAMs generated from the modular disulfides were characterised with a suite of surface analyses techniques and scanning near-field photolithography (SNP) was used to generate nanoscale patterns on their surfaces, thus demonstrating the suitability of these materials for nanofabrication.

Results and Discussion

Solid-phase synthesis: It was envisaged that a strategy reminiscent of solid-phase peptide synthesis could be adopted generate a variety of functionalised thiols for SAMs.[38–41] For the purposes of this synthesis, a solid-phase strategy is more efficient than solution-phase synthesis, because it allows excess of reagents to force high yields and simple washing steps obviates the need for purification of intermediates. Accordingly, two pegylated alkyldisulfides **1** and **2**, were chosen as synthetic targets, which are more stable to oxidation and reactions with electrophiles than the corresponding thiols, but are still able to form SAMs (Scheme 1). The SAMs generated from **1** would be able to provide a bulk bioresistant surface,[42,43] while in the featured areas, **2** would allow further chemical elaboration at the amino group. The latter disulfide also incorporated an additional PEG spacer to allow greater accessibility to this terminal moiety above the bulk surface of the SAM. Thus, a modular strategy was envisaged in which the more simple building blocks **3–5** were synthesised and then combined on the solid support **6**. It was also envisaged that the internal amide bonds of **1** and **2**, apart from acting as the link between the building blocks, would also impart improved SAM stability by virtue of lateral hydrogen bonding between the SAM units[44,45] in contrast to 11-mercaptoundecyl tri(ethylene) glycol (**7**), the material commonly used in the preparation of bioresistant SAM surfaces[20,24,26] which lacks the internal amide bond.

Synthesis of the pegylated building blocks **3** and **4** (Scheme 2) from triethylene glycol was acheived without chromatography,[46] via common intermediate **8**. Acetylation of **8** gave **9** followed by trifluoroacetic acid (TFA) acidolysis to generate building block **3**. Mesylation of **8** and displacement with sodium azide gave **10**, which on acidolysis revealed the azido–PEG acid **4** with the azido group functioning as a masked amine for solid-phase synthesis. The alkylthiol **5** was prepared from 11-bromoundecanol (Scheme 3), which on treatment with potassium phthalimide gave **11**. Activation of the alcohol of **11** and substitution with potassium thioacetate resulted in **12**, which on treatment with sodium methanethiolate[47] gave the free thiol **5**.

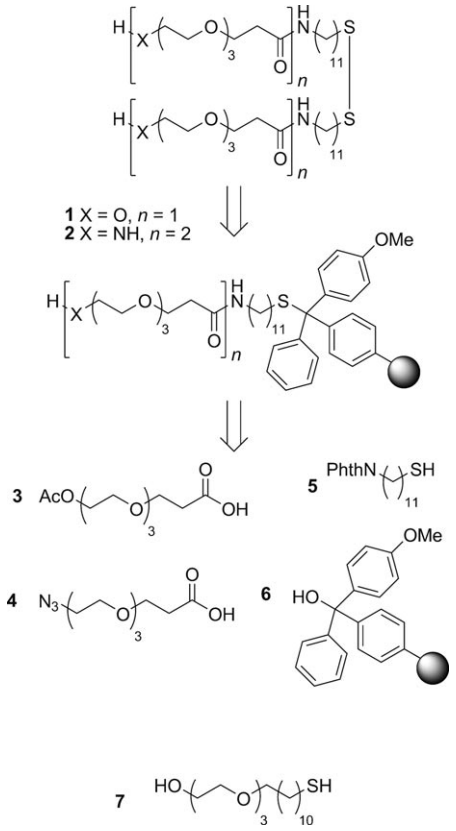

Scheme 1. Retrosynthetic outline for the solid-phase synthesis of pegylated alkanedisulfides **1** and **2**. The structure of 11-mercaptoundecyl tri(ethylene) glycol **7** is also included for comparison.

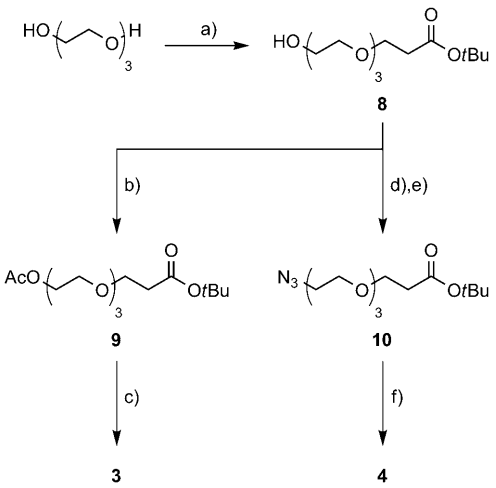

Scheme 2. Reagents and conditions: a) *tert*-Butyl acrylate, Na (cat.), THF, 18 h, 75%; b) Ac_2O, Et_3N, CH_2Cl_2, 16 h, 99%; c) 50% TFA, CH_2Cl_2, 2 h, 86%; d) mesyl chloride, Et_3N, CH_2Cl_2, 2 h; e) NaN_3, DMF, 7 d, 95% over 2 steps; f) 4 M HCl, 1,4-dioxane, 2 h, 80%.

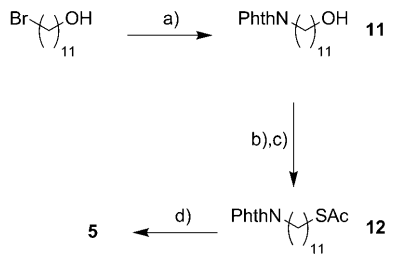

Scheme 3. Reagents and conditions: a) PhtNK, DMF, 60 °C, 4 h, 98 %; b) mesyl chloride, Et_3N, CH_2Cl_2, 2 h; c) AcSH, K_2CO_3, DMF, 15 h, 97 % over 2 steps; d) NaSMe, MeOH, 2 h, 94 %.

For the solid-supported synthesis (Scheme 4), the acid-labile 4-methoxytrityl polystyrene resin **6** commonly used for the immobilisation of thiols was employed.[48] The hydroxy resin was activated using thionyl chloride[49] and thiol component **5** attached to give **13**. Similar to a previously reported solid-phase strategy,[41] attachment through its S atom served to protect the thiol from reaction during the solid-phase assembly. On-resin hydrazinolysis of the phthalimide revealed the amine **14**. A portion of the amine resin **14** was treated with fluorenylmethyloxycarbonyl chloride (FmocCl) to give **15** and UV/Vis quantification of the subsequently cleaved piperidine–fulvene adduct, revealed a 53 % resin loading of the thiol relative to the original amount of hydroxytrityl groups on the resin, in agreement with previous reports with resin **6**.[48] To complete the synthesis of the target compound **1**, the acetoxy building block **3** was coupled to **14**, but this step was found to be slow. Even when the highly active coupling agent *N,N′*-tetramethylchloroformamidium hexafluorophosphate (TCFH) was used, 2.5 days was required for complete acylation (as determined by Kaiser tests). Deacetylation with hydrazine gave the hydroxy-functionalised **16**. Cleavage from the resin was affected with 5 % TFA and the crude material subjected to air oxidation to form the disulfide. Finally, purification by HPLC yielded the pure **1** with a 75 % overall yield based on the Fmoc quantification of the loaded aminoalkylthiol **14** (94 % average conversion per step).

For the synthesis of amino-functionalised disulfide **2**, the azido building block **4** was first coupled with the amine of **14**, which was also slow requiring 2.5 days for completion. A solid-phase version of the Staudinger reduction[50,51] gave the free amine to which the next pegylated unit could be attached and the azide reduced in a stepwise manner to give **17**. Cleavage and oxidation under similar conditions for **1** followed by HPLC purification gave **2** in 65 % yield based on the Fmoc quantification (95 % per step). It should be noted that although both **1** and **2** were isolated here as the disulfides for convenience, if desired, omission of the final air oxidation step would yield the free thiols.[48]

Stability of SAMs: As noted above, it was intended that incorporation of the amide bond would improve the stability of the SAMs of **1** and **2** compared to the widely used 11-mercaptoundecyl tri(ethylene) glycol (**7**). In order to assess this, the displacement of pegylated adsorbates by 16-hexade-

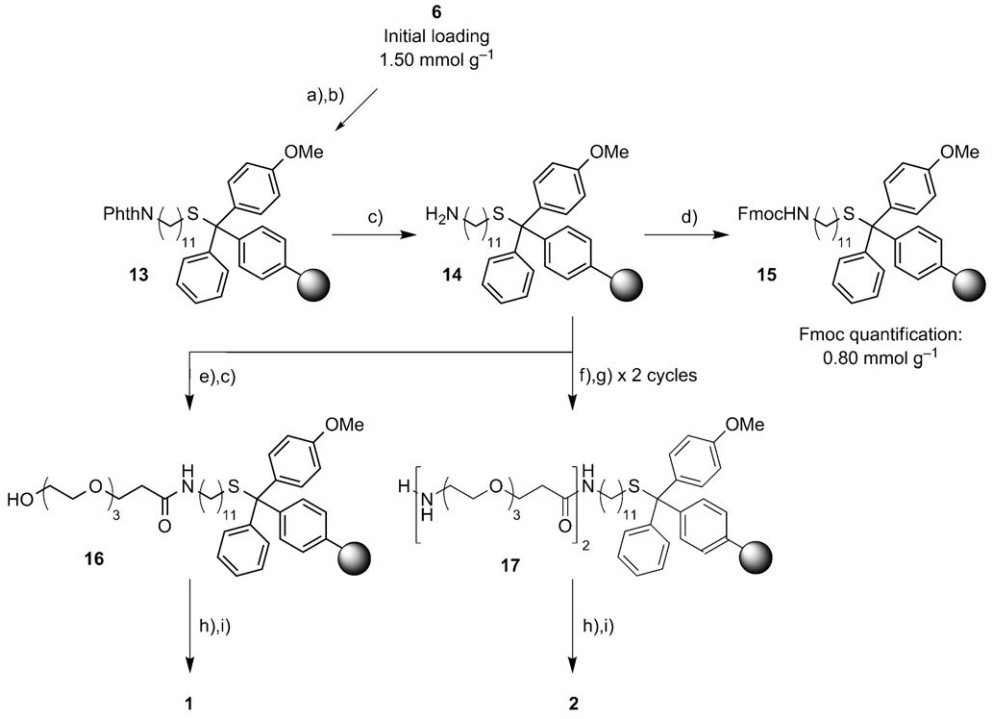

Scheme 4. Reagents and conditions: a) $SOCl_2$, CH_2Cl_2, 1 h; b) **5**, DIPEA, CH_2Cl_2, 2 h; c) 15 % N_2H_4, DMF/MeOH (8:2), 16 h; d) FmocCl, DIPEA, CH_2Cl_2/DMF (1:1), 2 h; e) **3**, TCFH, DIPEA, CH_2Cl_2/DMF (1:1), 65 h; f) **4**, TCFH, DIPEA, CH_2Cl_2/DMF (1:1), 65 h; g) Me_3P, H_2O, 1,4-dioxane/THF, 18 h; h) 5 % TFA, CH_2Cl_2, 3 min × 6 cycles; i) air, aq. $(NH_4)HCO_3$ pH 8–10, 16 h.

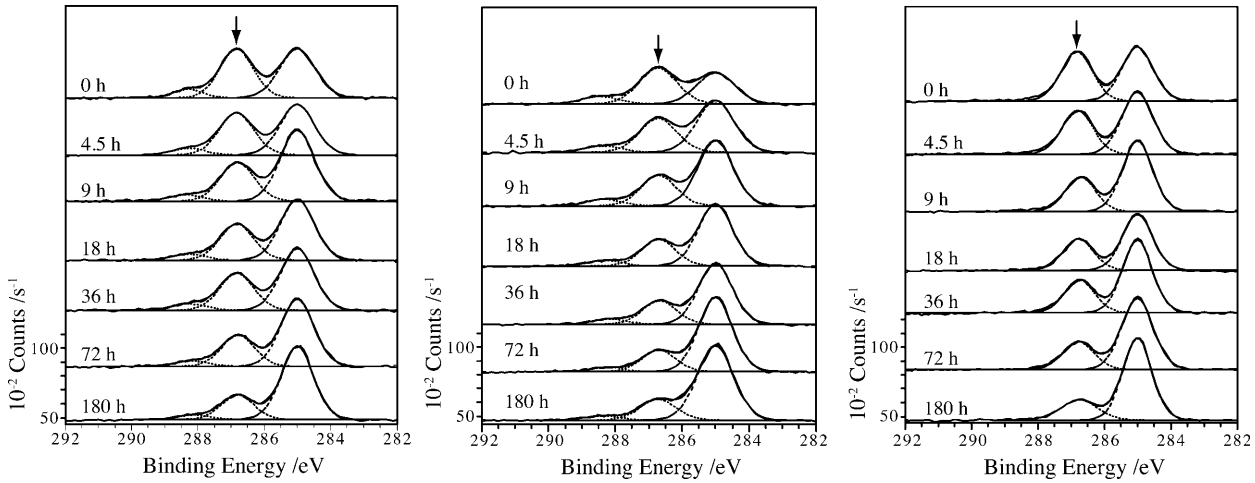

Figure 1. Typical XPS C1s spectra of films of a) **1**, b) **2** and c) **7** following immersion in the 16-hexadecanethiol for a range of durations. Arrows indicate the position of the CCO peak on each spectrum of the freshly prepared SAMs. Peak table of C1s binding energies derived from the fitting of XPS spectra can be found in supporting information (Table S1 in the Supporting Information).

canethiol was studied. Our hypothesis was that if the incorporation of amide groups into the adsorbate would confer greater stability on the resulting monolayer, then the rate of displacement should be slowed. The proportion of the SAM thiolates that were displaced by immersion in a 10 mM solution of 16-hexadecanethiol in ethanol over varying periods of time was readily quantified by XPS, following analysis of the C1s spectra (Figure 1 and Table S1 in the Supporting Information).

Spectra were first acquired for freshly prepared samples (0 h). In agreement with previously reported data,[52] the C1s spectrum of SAMs prepared from **7** exhibits two major components, one at a binding energy of ≈286.8 eV due to the ether unit (henceforth CCO), and one due to the carbon atoms in the alkyl chain (CCC), always adjusted to 285 eV. In comparison, spectra of films from **1** contain three peaks, attributable to CCO, CCC and NC=O (the latter at ≈288.3 eV). Films of **2** also include these three major peaks. Consideration of the molecular structure of **2** suggests that a peak may additionally be expected at 286.65 eV, due to the ammonium functional group. However, because of the close proximity of this peak to the main C1s peak, we did not attempt to resolve it during fitting. In comparison, C1s spectra of *n*-alkylthiols such as 16-hexadecanethiol consist of a single CCC component at 285 eV. C1s spectra were then acquired from films of **1**, **2** and **7** following immersion in 16-hexadecanethiol for a range of durations (Figure 1). If immersion of the pegylated SAMs in solutions of 16-hexadecanethiol leads to displacement of the pegylated adsorbate, it will thus be accompanied by an increase in the size of the CCC component in the C1s spectrum and a concomitant reduction in the size of the CCO component. In line with this, the spectra for films made from **1** showed a marked decrease in the area of this peak over time, while the CCC peaks (to the right of the CCO peak at 285 eV) show an increase, indicating that molecules in the film are gradually displaced by 16-hexadecanethiol over time. A decrease in the peak corresponding to the amide functionality together with the decrease in CCO is also observed and is consistent with this hypothesis. In the spectra for films of **2**, the CCO peak was initially greater than in **1** due to the increased size of the ether component in this molecule. This peak also underwent a similar decrease over time.

To quantify the changes observed in these data, the area of the CCO component relative to the area of the Au(4f 7/2) peak was calculated and normalised to the initial (0 h) value. The resulting data are plotted as a function of the immersion time (Figure 2). SAMs of the hydroxy-terminated monolayer of **1** yielded a larger ratio than that measured for a monolayer of **7** at all immersion times, suggesting enhanced stability, although when allowance is made for the error bars, it may be concluded that the improvement in stability is modest. This enhancement in stability is attributed

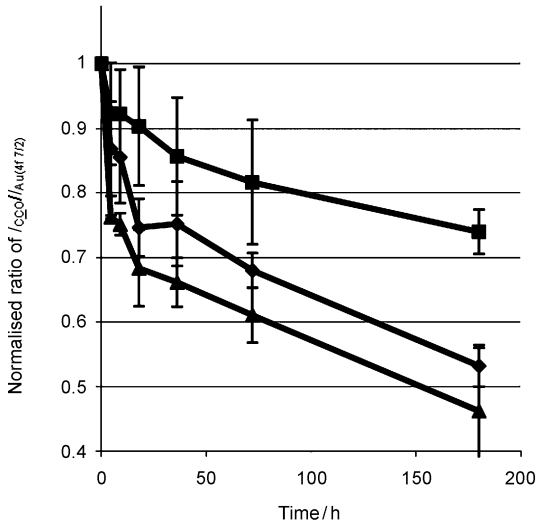

Figure 2. Graph of XPS CCO peak intensity ratio for the SAMs prepared from **1** (◆), **2** (■) and **7** (▲) against immersion time in a hexadecanethiol solution.

to the formation of lateral (intra-monolayer) hydrogen bonds between amide groups, which causes an increase in the desorption energy and hence reduces the rate-constant for desorption of thiolates from the gold surface in monolayers of **1** relative to that for **7**. At all immersion times, SAMs of **2** yielded a clearly larger CCO/Au4f ratio than was measured for monolayers of either **1** or **7**, indicating that they had a much greater resistance to displacement by hexadecanethiol. This was thought to be due to the capacity of **7** to form two lateral, intra-monolayer amide bonds, which is expected to yield a significant increase in the desorption enthalpy, reducing the rate of desorption from the surface. It is also possible that lateral hydrogen-bonding interactions between amine terminal groups may further contribute to the stabilisation of the monolayers. SAMs of both of the amide-bearing **1** and **2** were thus more stable than those formed from thiol **7**, and after 180 h, 49% and 75% of the thiolates from **1** and **2**, respectively, remained at the surface, compared to less than 35% in the SAM of **7**.

Resistance to protein adsorption: The SAMs of **1**, **2** and **7** were also assessed for their resistance to the non-specific adsorption of proteins by SPR (surface plasmon resonance) spectroscopy. Here, the change in SPR was measured as solutions of individual proteins were flowed over the SAMs followed by buffer solutions to desorb any loosely bound protein. The differences in the SPR response level after the buffer wash was used as an indicator of the amount of residual protein adsorbed to the surfaces, which was compared between the different SAMs.[42] Three test proteins were examined; bovine serum albumin (BSA), the acyl carrier protein BtrI from *Bacillus circulans* and phosphopantethienyl transferase Sfp from *Bacillus subtilis*,[53,54] which represent a range of protein types. The hydroxy-terminated SAMs from **1** that possessed the internal amide bond were found to possess marginally superior resistance to adsorption compared to hydroxy-terminated SAMs produced from **7** for all the proteins tested, confirming that these disulfides formed bioresistant monolayers (Figure 3). This difference in bioresistance may be due to the internal hydrogen-bonding resulting in a tighter packing of the hydrophobic alkyl chains and a reduction of their exposure to the proteins. As expected, the proteins adhered to SAMs from the amino-functionalised disulfide **2**, probably through electrostatic interactions since the termini of the SAMs present charged ammonium species under these physiological conditions. Indeed, such interactions are commonly used as a means of non-covalent protein immobilisation.[31,55] The SPR curve for **2** appears to differ slightly from those of **1** and **7** in the association region. The reason for this is not certain, although the most likely explanation would be that it results from the charged nature of the terminal group for adsorbate **2** (an ammonium ion, compared to the hydroxyl termini of the other two systems studied).

Scanning near-field photolithography (SNP): In respect to the further aim of developing functionalised nano-patterned

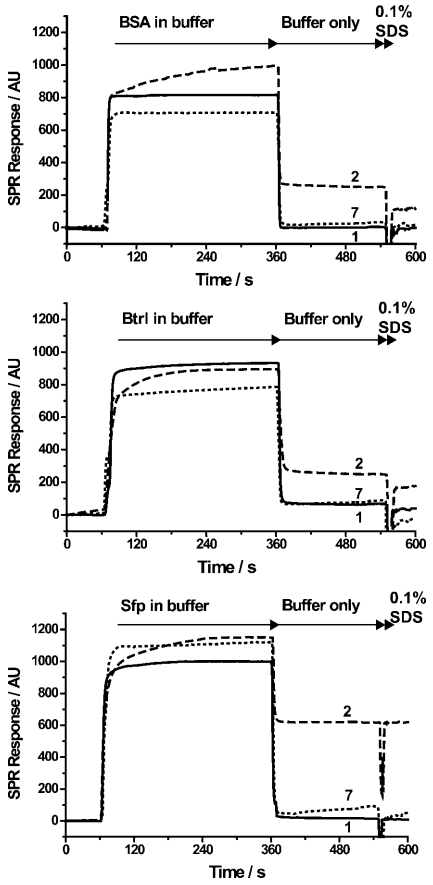

Figure 3. SPR sensograms of SAMs composed from **1**, **2** and **7** with exposure to the proteins: a) BSA, b) BtrI and c) Sfp.

surfaces employing these disulfides, hydroxy-terminated SAMs composed of **1** were subjected to SNP. Light with a wavelength of 244 nm was coupled to the optical fiber probe and the sample exposed to the optical near field associated with the aperture at its apex. This enabled the photooxidation of the thiolates in the SAM to the corresponding sulfonates, which could be displaced subsequently with a second thiol.[14] Firstly, an arrangement of dots was fabricated by holding the probe stationary at each location in a 6×6 matrix of points. The sample was then immersed in a solution of 16-hexadecanethiol. After rinsing with ethanol and drying, the friction force microscopy (FFM) image (Figure 4a) revealed dark contrast on the exposed regions compared to the rest of the surface, as expected, due to the reduced coefficient of friction in these areas. Figure 4b shows an FFM image of a pattern formed by writing six parallel lines into a SAM of **1**, and subsequently immersing the sample in a solution of 3-mercaptopropanoic acid. The exposed regions now exhibited brighter contrast than the surrounding material; again consistent with existing literature that shows that the coefficients of friction of hydroxy-terminated SAMs are 50% those of carboxylic acid terminated monolayers. Finally, the pattern formed by writing into a SAM of **1** and incorporation of **2** into the exposed regions

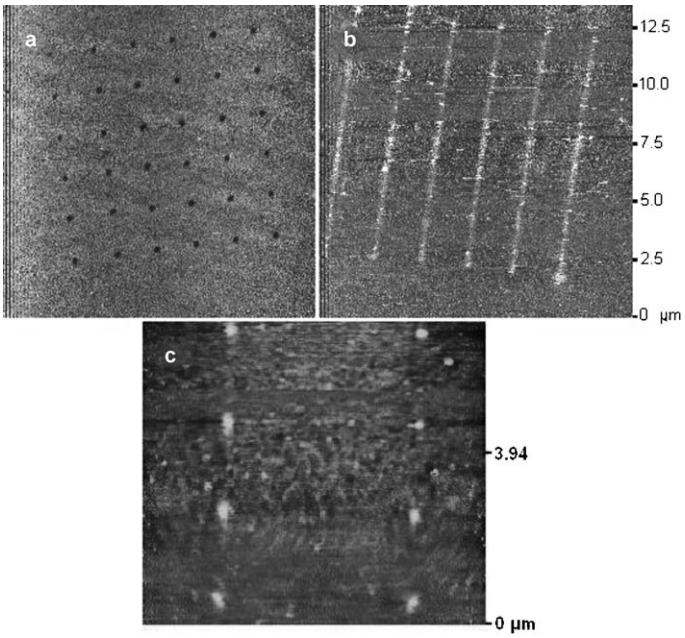

Figure 4. Friction force microscopy images of SAMs of **1** with features generated by SNP followed by displacement of the oxidised thiol with a) 16-hexadecanethiol, b) 3-mercaptopropionic acid and c) **2**.

was imaged using FFM (Figure 4c). In this case the dots exhibit brighter contrast, which may result from the electrostatic interaction between the negatively charged probe and positive charges on the ammonium terminated regions (the outer surface of a silicon nitride probe is composed of a thin layer of silicon dioxide, which is expected to carry a net negative charge). In all cases submicron features with a mean full width at half maximum height (fwhm) of ≈190 nm were generated. These data indicate that oxidation down to the S atom was successful and the entire molecule was displaced by the incoming thiol, giving rise to the complimentary lateral force images after exposure to 16-hexadecanethiol or 3-mercaptopropionic acid (Figure 4a and b).

SAM **18**, presenting a "dashed" pattern of the ammonium-terminated features from disulfide **2** on a bulk surface of the hydroxy-pegylated **1**, was then used to demonstrate the immobilisation of proteins by both covalent and non-covalent means (Scheme 5). Here, the electrostatic interactions mentioned above were exploited to immobilise immunoglobulin G (IgG) as a model protein. For covalent binding, **18** was treated with the cross-linking agent glutaraldehyde to generate SAMs with aldehyde-functionalised features **19**. IgG was then covalently immobilised by imine formation. The surfaces with the immobilised IgG were then imaged by AFM in tapping mode for more accurate height measurements. The protein nanofeatures that were generated had a mean fwhm of 180 nm for the electrostatically immobilised protein and 178 nm for the covalent immobilisation (Figure 5). Also, the electrostatically bound IgG features had a height of 3.0 nm while the glutaraldehyde-bound protein features had a height of 3.5 nm compared to the bulk

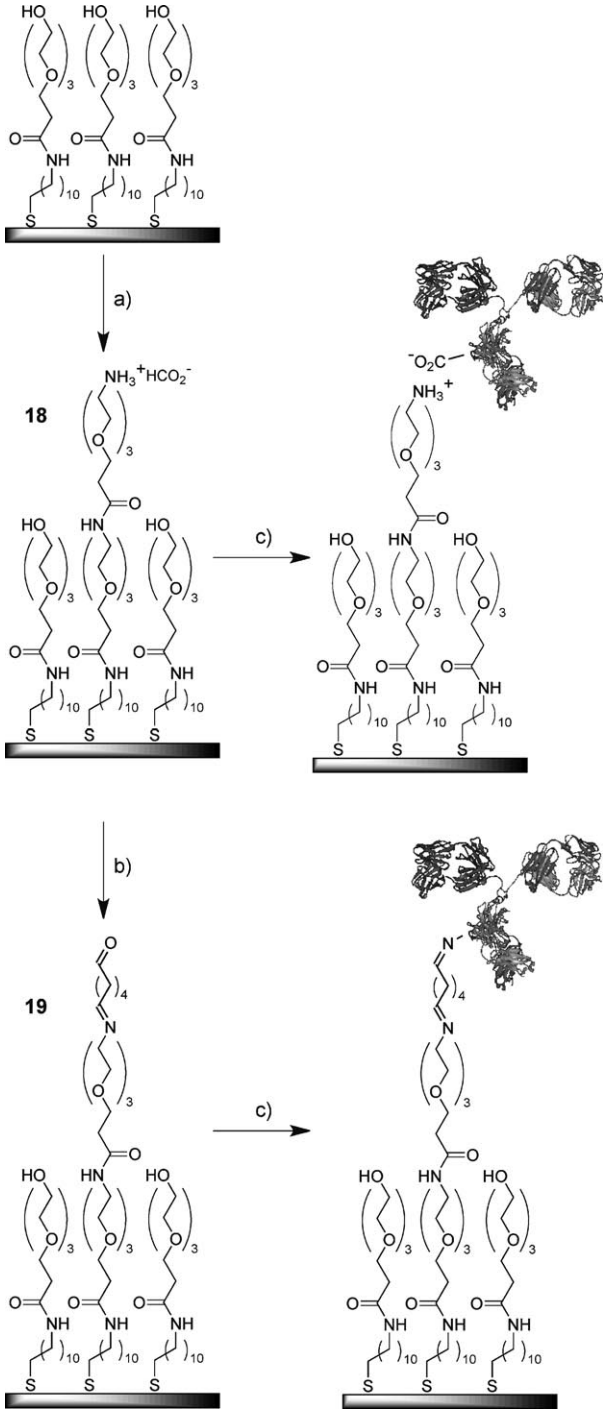

Scheme 5. Reagents and conditions: a) SNP at 244 nm, then **2**, EtOH, 18 h; b) 25% aq. glutaraldehyde, 30 min; c) IgG, PBS pH 7.4, 2.5 h.

surface, consistent with previous results.[56] In comparison, the features prior to protein immobilisation gave a small height decrease of ≈0.2 nm, possibly due to the looser packing of the incoming pegylated units. Thus, these experiments demonstrate that patterns of nanoscale protein features could be generated on these materials.

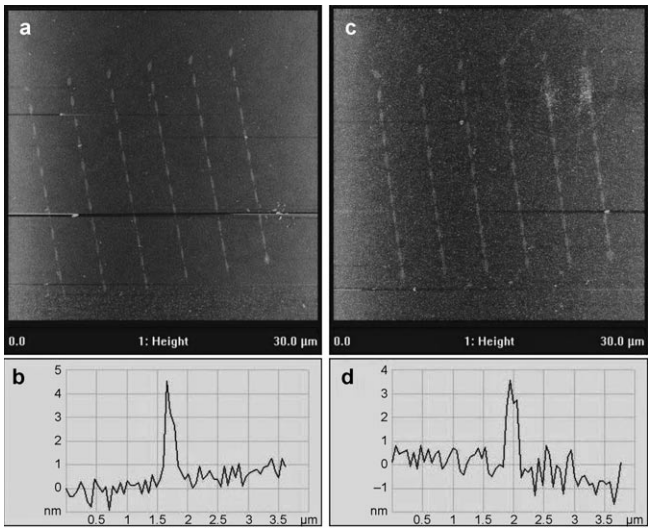

Figure 5. Tapping mode AFM images of SAMs with IgG immobilised through a) electrostatic interactions to **18** with b) a topographic plot of a representative feature; and c) imine formation to **19** with d) a topographic plot of a representative feature.

Conclusion

In summary, a synthetically expedient method for the assembly of functionalised pegylated alkyldisulfides employing an alternative solid-phase synthetic strategy was successfully demonstrated, providing the disulfides in high yields and requiring only one chromatographic purification during the final isolation. Up until now researchers in this field have primarily relied on a limited number of alkyl thiols that are commercially available. However, it is envisaged that by using the simple building blocks and solid-phase methodology presented here, and together with other strategies, even laboratories with little synthetic experience will be able to prepare bespoke pegylated thiols in a similar way to which peptides are synthesised. Indeed, by harnessing the full spectrum of available solid-phase and combinatorial synthetic methodologies, it is expected that a plethora of SAM materials with functional groups not previously studied will now become accessible.

Further, SAMs of both the synthesised disulfides **1** and **2** were characterised and shown to possess a number of desirable properties which were relevant for biological applications. These SAMs, which incorporated internal amide linkages, had improved stability towards displacement by hexadecanethiol when compared to the more commonly used comparison material **7** which lacked the amide moiety. The SAMs prepared from the hydroxy-functionalised disulfide **1** demonstrated at least equal biocompatibility in comparison to **7** as determined by SPR for a range of proteins. Additionally, these SAMs are amenable to SNP that allowed the generation of features of less than 190 nm. The fabrication of a SAM of **1** with amino-presenting features of **2** allowed the generation of protein patterns through both covalent and non-covalent immobilisation methods, a significant result since these promise to be effective methods for the fabrication of protein nano-features.[20,56–59] It is expected that under optimum conditions, truly nanoscopic feature sizes as small as 9 nm may be fabricated.[20]

The work shown in this report will be useful in the future development of biomolecular "nanoarrays" for high throughput screening and wider applications in biomedical diagnostics, biosensors, organic material electronics and the assembly of more complex three-dimensional structures.[60] Nevertheless, the nanopatterned SAMs described can potentially find more immediate use in the investigation of cell biology mediated by cell surface interactions. These surfaces may also be a route to the isolation of single molecules in the study of single molecule dynamics and enzymology.

Experimental Section

Materials and equipment: 4-Methoxytrityl hydroxide polystyrene resin with an initial loading of 1.5 $mmol g^{-1}$ was purchased from Iris Biotech (Marktredwitz, Germany) All DMF used was of peptide synthesis grade from Rathburn Chemicals (Walkerburn, UK). Substrates used were borosilicate glass slides (Chance number 2 thickness, 64 mm × 22 mm). Pegylated thiol **7** was synthesised according to a published procedure.[52] All EtOH used was of HPLC grade and degassed prior to use. Hexadecanethiol and mercaptopropionic acid were purchased from Sigma–Aldrich (Gillingham, UK). BSA and IgG from human serum was purchased from Sigma–Aldrich and reconstituted in 100 mM phosphate buffered saline (PBS). BtrI and Sfp were expressed and purified as previously described[53] with BtrI in 50 mM HEPES buffer (pH 7.0), 50 mM NaCl, 2 mM dithiothreitol, 0.5 mM EDTA and Sfp in 50 mM HEPES buffer (pH 7.6), 200 mM NaCl. These proteins were donated by Dr. J. L. Thirlway (Manchester Interdisciplinary Biocentre, University of Manchester). All the proteins were used at a concentration of 100 $\mu g m L^{-1}$ for the SPR experiments.

Equipment: Reversed-phase HPLC was conducted on a Varian ProStar 320 with a Phenomenex Gemini C18 5 µm 250 × 10 mm column using water with 0.1% formic acid and MeCN with 0.1% formic acid as eluents. A gradient from 5 to 100% $MeCN/HCO_2H$ from 0–20 min followed by an isocratic elution of 100% $MeCN/HCO_2H$ from 20–37 min was used in all cases. Biocompatibility studies were carried out using a Biacore 3000 SPR Instrument (GE Healthcare UK, Little Chalfont, UK) with an automatic sample changer maintained at 25 °C. XPS was carried out using a Kratos Axis Ultra DLD (Kratos Analytical, Manchester, UK) with monochromated $Al_{K\alpha}$ X-ray source. SAM samples were analysed by contact mode lateral force microscopy (LFM) using a ThermoMicroscopes Explorer and in tapping mode with a Nanoscope IIIa atomic force microscope (Veeco, Cambridge, UK). SNP was performed using ThermoMicroscopes Aurora III NSOM systems (Veeco).

***tert*-Butyl 12-hydroxy-4,7,10-trioxadodecanoate (8)**: This compound was synthesised based on a previous procedure.[46] Sodium (200 mg, 8.7 mmol) was dissolved in anhydrous triethylene glycol (126 mL, 940 mmol) under N_2 and anhydrous THF (500 mL) was added. *tert*-Butyl acrylate (49 mL, 334.5 mmol) was dissolved in anhydrous THF (500 mL) under N_2 and added dropwise over 5 h to the glycol solution. The entire mixture was stirred under N_2 until all the acrylate was consumed (≈12 h). The mixture was adjusted to pH 7–8 by dropwise addition of 1 M aq. HCl (≈8 mL) and the THF evaporated under reduced pressure. The residual oil was redissolved in EtOAc (1 L) and extracted with brine (1 L once then 0.4 L once). The organic layer was dried with Na_2SO_4, evaporated under reduced pressure and the residual oil dried in vacuo to yield a pale yellow oil (69.47 g, 249.6 mmol, 75% with less than 1% diester by NMR). $R_f = 0.33$ (EtOAc); IR (BaF_2): $\tilde{\nu} = 3438$ (OH), 2872 (alkyl), 1727 (COO), 1368 (CH_2O), 1161, 1119 cm^{-1} (COO or CH_2O); ^1H NMR (400 MHz, $CDCl_3$): $\delta = 1.41$ (s, 9H; CH_3), 2.48 (t, $J = 7$ Hz, 2H; 2-CH_2),

2.67 (br s, 1H; O*H*), 3.65–3.73 ppm (m, 14H; 3,5,6,8,9,11,12-CH_2O); ^{13}C NMR (100 MHz, $CDCl_3$): δ = 28.2 (CCH_3), 36.3 (2-*C*H_2CO), 61.8 (12-*C*H_2OH), 67.0 (3-*C*H_2O), 70.4, 70.6, 70.7 (5,6,8,9-*C*H_2O), 72.6 (11-*C*H_2O), 80.6 (*C*CH_3), 171.0 ppm (*C*OO); MS (CI): *m/z* (%): 223 (20) $[M-t\text{Bu}+H]^+$, 240 (100) $[M-t\text{Bu}+NH_4]^+$, 296 (40) $[M+NH_4]^+$.

***tert*-Butyl 12-acetoxy-4,7,10-trioxadocecanoate (9)**: The pegylated ester **8** (5567 mg, 20 mmol) was dissolved in CH_2Cl_2 (distilled, 30 mL) and Et_3N (4181 μL, 30 mmol) was added followed by Ac_2O (2363 μL, 25 mmol). A silica drying tube was attached and the mixture stirred for 16 h after which water (50 mL) was added and the mixture was extracted Et_2O (50 mL × 3). The organic layer dried with Na_2SO_4, evaporated under reduced pressure and dried in vacuo to yield the desired acetate as a colourless oil (6331 mg, 19.76 mmol, 99%). R_f = 0.66 (hexane:EtOAc, 1:3); IR (BaF_2): $\tilde{\nu}$ = 2882 (alkyl), 1732 (COOR), 1367 (Me), 1244 (COOR), 1123 cm^{-1} (ROR); ^{1}H NMR (400 MHz, $CDCl_3$): δ = 1.44 (s, 9H; C-(C*H*$_3$)$_3$), 2.07 (s, 3H; C*H*$_3$CO), 2.50 (t, *J* = 7 Hz, 2H; 2-C*H*$_2$CO), 3.55–3.75 (m, 12H; 3,5,6,8,9,11-C*H*$_2$O), 4.21 ppm (t, *J* = 7 Hz, 2H; 12-CO$_2$C*H*$_2$); ^{13}C NMR (75 MHz, $CDCl_3$): δ = 21.4 (*C*H$_3$CO), 28.5 (C-(*C*H$_3$)$_3$), 36.6 (2-*C*H$_2$CO), 64.0 (3-*C*H$_2$O), 67.3 (12-CO$_2$*C*H$_2$), 69.5 (11-*C*H$_2$O), 70.8, 71.0 (5,6,8,9-*C*H$_2$O), 80.9 (*C*(CH$_3$)$_3$), 171.3 (1-*C*O$_2$), 171.4 ppm (CH$_3$*C*O); MS (CI): *m/z* (%): 338 (100) $[M+NH_4]^+$; HRMS: *m/z* calcd for $[M+NH_4]^+$: 338.2173; found 338.2172 (δ = 0.4 ppm).

12-Acetoxy-4,7,10-trioxadocecanoic acid (3): The acetoxy ester **9** (6326 mg, 19.75 mmol) was dissolved in CH_2Cl_2 (50 mL), TFA (50 mL) was added and the mixture was stirred for 2 h. Subsequently, the solution was evaporated under reduced pressure and the residual oil was redissolved in CH_2Cl_2 (100 mL) and stirred with Amberlyst A-21 for 1 h. The resin was filtered and the filtrate evaporated under reduced pressure to give **3** as a pale yellow oil (4486 mg, 16.98 mmol, 86%). R_f = 0.05 (hexane:EtOAc, 1:3); IR (BaF_2) $\tilde{\nu}$ = 3483 (COOH), 2878 (alkyl or COOH), 1737 (COOR or COOH), 1248 (COOR or COOH), 1111 cm^{-1} (ROR); ^{1}H NMR (400 MHz, $CDCl_3$): δ = 2.06 (s, 3H; C*H*$_3$CO), 2.62 (t, *J* = 6 Hz, 2H; 2-C*H*$_2$CO), 3.55–3.71 (m, 10H; 5,6,8,9,11-*C*H$_2$O), 3.75 (t, *J* = 6 Hz, 2H; 3-*C*H$_2$O), 4.21 ppm (t, *J* = 5 Hz, 2H; 12-CO$_2$C*H*$_2$); ^{13}C NMR (100 MHz, $CDCl_3$): δ = 21.1 (*C*H$_3$CO), 34.9 (2-*C*H$_2$CO), 63.7 (12-CO$_2$*C*H$_2$), 66.4 (3-*C*H$_2$O), 69.2 (11-*C*H$_2$O), 70.5, 70.6, 70.7 (5,6,8,9-*C*H$_2$O), 171.4 (CH$_3$*C*O), 176.3 ppm (1-*C*O$_2$H); MS (ES+): *m/z* (%): 287 (100) $[M+Na]^+$; HRMS: *m/z* calcd for $[M+Na]^+$: 287.1101; found 287.1094 (δ = 2.5 ppm).

***tert*-Butyl 12-azido-4,7,10-trioxadocecanoate (10)**: A solution of hydroxy–PEG ester **8** (9116 mg, 32.75 mmol) and Et_3N (9220 μL, 66.15 mmol) in CH_2Cl_2 (distilled, 50 mL) was cooled in an ice bath with a $CaCl_2$ drying tube. Mesyl chloride (3800 μL, 49.10 mmol) was added dropwise while stirring and the mixture was stirred at RT for a further 2.5 h. The mixture was reduced to a small volume under reduced pressure, water (350 mL) was added and the suspension was extracted with EtOAc (250 mL × 3). The organic layers were combined and dried with Na_2SO_4 then evaporated under reduced pressure to yield the mesylate as a yellow oil. This oil was redissolved in DMF (100 mL), NaN_3 (6387 mg, 98.25 mmol) and the suspension was stirred for 7 d. The mixture was reduced to a small volume under reduced pressure, water (200 mL) was added and extracted with Et_2O (150 mL × 2). The organic layers were combined, dried with Na_2SO_4, evaporated under reduced pressure and dried in vacuo to yield the desired compound as a pale yellow oil (9460 mg, 31.19 mmol, 95%). R_f = 0.59 (EtOAc); IR (BaF_2): $\tilde{\nu}$ = 2865 (alkyl), 2103 (N_3), 1722 (COOR), 1158 (COOR), 1119 cm^{-1} (ROR); ^{1}H NMR (400 MHz, $CDCl_3$): δ = 1.44 (s, 9H; C*H*$_3$), 2.50 (t, *J* = 7 Hz, 2H; 2-C*H*$_2$), 3.39 (t, *J* = 5 Hz, 2H; 12-C*H*$_2$), 3.57–3.80 ppm (m, 12H; 3,5,6,8,9,11-C*H*$_2$); ^{13}C NMR (100 MHz, $CDCl_3$): δ = 28.2 (CCH_3), 36.4 (2-*C*H$_2$CO), 50.8 (12-*C*H$_2$N$_3$), 67.0 (3-*C*H$_2$O), 70.2, 70.5, 70.8 (t; 5,6,8,9,11-*C*H$_2$O), 80.7 (*C*CH_3), 171.1 ppm (*C*OO); MS (CI): *m/z* (%): 265 (100) $[M-t\text{Bu}+NH_4]^+$, 321 (80) $[M+NH_4]^+$; HRMS: *m/z* calcd for $[M+NH_4]^+$: 321.2132; found 321.2125 (δ = 2.3 ppm).

12-Azido-4,7,10-trioxadocecanoic acid (4): The azido–PEG ester **10** (2000 mg, 6.59 mmol) was stirred with 4 M HCl in 1,4-dioxane (10 mL) for 12 h and the mixture was then evaporated under reduced pressure. The residual oil was redissolved in CH_2Cl_2 (10 mL) and stirred with Amberlyst A-15 resin (2 g) for 15 min. The solution was eluted and the resin was washed with CH_2Cl_2 (10 mL × 3). The organic phases were combined and evaporated under reduced pressure and the residue dried in vacuo to yield **4** as a brown oil (1304 mg, 5.28 mmol, 80%). R_f = 0.15 (hexane:EtOAc, 1:2); IR (BaF_2): $\tilde{\nu}$ = 3343 (COOH), 2871 (alkyl), 2109 (N_3), 1727 (COOH), 1182 (COOH), 1120 cm^{-1} (ROR); ^{1}H NMR (400 MHz, $CDCl_3$): δ = 2.66 (t, *J* = 6 Hz, 2H; 2-C*H*$_2$CO), 3.40 (t, *J* = 5 Hz, 2H; 12-C*H*$_2$N$_3$), 3.56–3.83 (m, 12H; 3,5,6,8,9,11-C*H*$_2$O), 9.06 ppm (br s, 1H; COO^{13}C NMR (100 MHz, $CDCl_3$): δ = *C*H$_2$O), 70.1, 70.5, 70.7 (5,6,8,9,11-*C*H$_2$O), 176.2 ppm (*C*OOH); MS (ES+): *m/z* (%):270 (100) $[M+Na]^+$, 286 (60) $[M+K]^+$; HRMS: *m/z* calcd for $[M+Na]^+$: 270.1060; found 270.1058 (δ = 0.9 ppm).

11-(*N*-Phthalimido)undecan-1-ol (11): 11-Bromoundecanol (5008 mg, 20 mmol) and potassium phthalimide (4078 mg, 22 mmol) were mixed in DMF (100 mL) and refluxed at 60 °C for 4 h. The mixture was evaporated to a small volume under reduced pressure, resuspended in $CHCl_3$ (25 mL) and filtered through a celite bed. The filtrate was evaporated under reduced pressure to yield the desired product as a white solid (6215 mg, 19.58 mmol, 98%). R_f = 0.37 (hexane:EtOAc, 2:1); m.p. 85 °C (lit.[61] 85–86 °C); IR (BaF_2): $\tilde{\nu}$ = 3344 (OH), 2926 (alkyl), 2848 (alkyl), 1717 (imide), 1399 (alkyl), 1057 (OH), 725 cm^{-1} (aryl); ^{1}H NMR (300 MHz, $CDCl_3$): δ = 1.10–1.40 (m, 14H; 3–9-C*H*$_2$), 1.42–1.75 (m, 4H; 2,10-C*H*$_2$), 3.56–3.75 (m, 4H; 1,11-C ppm; ^{13}C NMR (75 MHz, $CDCl_3$): δ = 25.8, 26.9, 28.7, 29.3, 29.5 (d), 29.6 (3–10-*C*H$_2$), 32.9 (2-*C*H$_2$), 38.2 (11-*C*H$_2$N), 63.2 (1-*C*H$_2$OH), 123.3 (2,5-Phth), 132.3 (1,6-Phth), 134.0 (3,4-Phth), 168.6 ppm (*C*ON); MS (ES+): *m/z* (%): 381 (100) $[M+Na+MeCN]^+$, 657 (50) $[2M+Na]^+$.

1-[11-(*N*-Phthalimido)]undecyl thioacetate (12): Compound **11** (2365 mg, 7.45 mmol) and Et_3N (1740 μL, 12.50 mmol) were dissolved in CH_2Cl_2 (25 mL). The solution was cooled in an ice bath, mesyl chloride (774 μL, 10 mmol) was added dropwise while stirring and the mixture was stirred at RT for a further 2 h. CH_2Cl_2 (50 mL) and Et_2O (25 mL) were added to the mixture and the resulting solution was extracted with 0.5 M aq. HCl (50 mL × 2), water (50 mL) and 5% w/v $NaHCO_3$ aq. solution (100 mL). The organic layer was dried with $MgSO_4$ and evaporated under reduced pressure to give the desired mesylate as a yellow oil which solidified on standing to a pale yellow solid. This was added to a vigorously stirring mixture of AcSH (620 μL, 8.70 mmol) and K_2CO_3 (1500 mg, 10.85 mmol) in DMF (50 mL) and stirred for 15 h. The suspension was reduced to a small volume under reduced pressure and the residue was resuspended with $CHCl_3$ (50 mL). This was extracted with water (150 mL × 2), 0.5 M aq. HCl (100 mL × 2) and 5% w/v $NaHCO_3$ aq. solution (150 mL × 3), dried with $MgSO_4$ and evaporated under reduced pressure to yield the thioacetate as a buff semi-crystalline solid (2728 mg, 7.26 mmol, 97%). R_f = 0.47 (hexane:EtOAc, 6:1); m.p. 78 °C; IR (BaF_2): δ = 2918 (alkyl), 2851 (alkyl), 1698 (CONCO and COS), 1467 (aryl), 1407 cm^{-1} (aryl); ^{1}H NMR (400 MHz, $CDCl_3$): δ = 1.15–1.45 (m, 14H; 3–9-C*H*$_2$), 1.54 (tt, *J* = 7, 7 Hz, 2H; 10-C*H*$_2$), 1.66 (tt, *J* = 7, 7 Hz, 2H; 2-C*H*$_2$), 2.31 (s, 3H; SCOC*H*$_3$), 2.85 (t, *J* = 7 Hz, 2H; 1-C*H*$_2$COS), 3.67 (t, *J* = 7 Hz 2H; NC*H*$_2$), 7.70 (dd, *J* = 3, 5 Hz, 2H; ppm Hz,^{1}H NMR : δ = 2,5-Phth), 132.3 (1,6-Phth), 134.0 (3,4-Phth), 168.6 (*C*ON), 196.3 ppm (*C*OS); MS (ES+): *m/z* calcd: 376 (85) $[M+H]^+$, 393 (25) $[M+NH_4]^+$, 768 (100) $[2M+NH_4]^+$; HRMS: *m/z* calcd for $[M+NH_4]^+$: 393.2206; found 393.2205 (δ = 0.4 ppm).

11-(*N*-Phthalimido)undecane-1-thiol (5): The thioacetate **12** (2306 mg, 6.45 mmol) was suspended in MeOH (anhydrous, degassed, 60 mL) under an inert atmosphere. Separately, NaSMe (456 mg, 6.50 mmol) was dissolved in MeOH (anhydrous, degassed, 6.5 mL) under an inert atmosphere and added to the thioacetate suspension. The mixture was stirred for 2 h during which the solids were observed to gradually dissolve and the reaction was quenched with 0.1 M aq. HCl (140 mL) and extracted twice with Et_2O (degassed, 75 mL). The organic layer was dried with $MgSO_4$, evaporated under reduced pressure and dried in vacuo to give **5** an oil, which solidified into a buff solid which was pure by NMR spectroscopy (2031 mg, 6.09 mmol, 94%). R_f = 0.57 (hexane:EtOAc, 4:1); IR (BaF_2): $\tilde{\nu}$ = 2925, 2851 (alkyl), 1713 (CONCO), 1393, 1365 cm^{-1} (SH or alkyl); ^{1}H NMR (400 MHz, $CDCl_3$): δ = 1.15–1.45 (m, 14H; 3–9-C*H*$_2$), 1.54–1.73 (m, 4H; 2,10-C*H*$_2$), 2.51 (td, *J* = 7, 7 Hz, 2H; 1-C*H*$_2$S), 3.67 (t, *J* = 7 Hz, 2H; NC*H*$_2$), 7.70 (dd, *J* = 3, 5 Hz, 2H; ppm Hz^{13}C NMR : δ =

2,5-Phth), 132.3 (1,6-Phth), 134.0 (3,4-Phth), 168.6 ppm (*C*ON); MS (ES+): *m/z* (%): 334 (100) $[M+H]^+$; HRMS: *m/z* calcd for $[M+H]^+$: 334.1835; found 334.18.40 ($\delta = 1.4$ ppm).

11-(*N*-Phthalimido)undecyl 1-thio-(4-methoxytrityl) polystyrene resin (13): Resin **6** (2 g, 3.0 mmol) was placed in a sealed sintered glass column and purged with N_2. $SOCl_2$ (330 μL, 4.53 mmol) was dissolved in CH_2Cl_2 (distilled, 9 mL) and added to the resin. The mixture was shaken for 1 h, the resin drained by applying N_2 pressure to the top of the column and washed with CH_2Cl_2 (distilled, 10 mL × 3). Thiol **5** (1250 mg, 3.75 mmol) and *N*,*N*-diisopropylethylamine (DIPEA; 2080 μL, 12.02 mmol) were dissolved in CH_2Cl_2 (distilled, 9 mL) then added to the resin and shaken for 2 h. The resin was drained, washed with CH_2Cl_2/MeOH/DIPEA (17:2:1, 10 mL × 3), CH_2Cl_2, MeOH, CH_2Cl_2, MeOH and Et_2O (10 mL × 3 each solvent in sequence). The resin was dried in vacuo and gave a negative result to the ninhydrin test.[62]

11-Aminoundecyl-1-thio-(4-methoxytrityl) polystyrene resin (14): The phthalimido-resin (200 mg) was shaken with 15% v/v $N_2H_4{\cdot}H_2O$ in DMF/CH_2Cl_2 (8:2, 1.5 mL) for 16 h. The solution removed and the resin washed with DMF, CH_2Cl_2, DMF, CH_2Cl_2 (3 mL × 3 each solvent in order) and dried in vacuo.

***N*-Fmoc-11-aminoundecyl-1-thio-(4-methoxytrityl) polystyrene resin (15)**: The aminoundecyl resin **7** (5 mg) was mixed for 2 h with CH_2Cl_2 (100 μL) containing DIPEA (5.2 μ, 30 μmol) and FmocCl (3.9 mg, 15 μmol). The resin was rinsed with DMF, CH_2Cl_2, DMF, CH_2Cl_2 (3 mL × 3 each solvent in order) and dried in vacuo to give a resin which yielded a negative ninhydrin test result and an Fmoc loading[63] of 0.80 mmolg^{-1} (53% over 3 steps relative or hydroxy-resin loading).

11-(12-Hydroxy-4,7,10-trioxadocecamido)undecyl-1-thio-(4-methoxytrityl) polystyrene resin (16): The acetoxy acid **3** (134 mg, 507 μmol) was dissolved in CH_2Cl_2/DMF (1:1, 800 μL), DIPEA was added (262 μL, 1514 μmol) and the mixture was cooled in an ice bath. TCFH (142 mg, 500 μmol) was added to the cooled solution, gently swirled for 2 min and the entire solution was added to the aminoundecyl resin **7** (316 mg, ≈250 μmol). The reaction was shaken for 65 h at RT, and the resin was drained, washed with DMF, CH_2Cl_2, DMF, CH_2Cl_2, Et_2O (3 mL × 3 each solvent in order) and dried in vacuo to give a resin which returned a negative ninhydrin test result. This resin was shaken with 15% v/v $N_2H_4{\cdot}H_2O$ in DMF/CH_2Cl_2 (8:2, 2 mL) for 16 h. The solution removed and the resin washed with DMF, CH_2Cl_2, DMF, CH_2Cl_2 (3 mL × 3 each solvent in order) and dried in vacuo.

Di-1-[11-(12-hydroxy-4,7,10-trioxadocecamido)undecyl]disulfide (1): The hydroxy-pegylated resin **16** above (~250 μmol) was mixed with 5% TFA v/v in CH_2Cl_2 (1 mL) for 3 min and the solution was eluted. This was repeated for a total of six cycles; the eluents were combined and evaporated under reduced pressure. The residual oil was resuspended in 0.1 M aq. $(NH_4)HCO_3$ (20 mL) and air was bubbled through the mixture until disulfide formation was complete (≈16 h). The mixture was lyophilised and purified by RP-HPLC, the desired fractions were combined and lyophilised to yield the desired product as a white solid (132 mg, 65% overall yield based on original Fmoc-resin loading). HPLC (256 nm) 24.5 min; ^{1}H NMR (400 MHz, CD_3OD): $\delta = 1.25$–1.57 (m, 32H; 3–10-CH_2), 1.68 (tt, $J = 7$, 7 Hz, 4H; 2-CH_2), 2.43 (t, $J = 7$ Hz, 4H; 2′-CH_2CO), 2.68 (t, $J = 7$ Hz, 4H; 1-CH_2S), 3.17 (t, $J = 7$ Hz, 4H; 11-CH_2N), 3.56 (t, $J = 5$ Hz, 4H; 11′-CH_2O), 3.59–3.69 (m, 20H; 5′,6′,8′,9′,12′-CH_2O), 3.72 ppm (t, 4H; $J = 5$, 3′-CH_2O); ^{13}C NMR (100 MHz, CD_3OD): $\delta = 28.0$ (9-*C*H_2), 29.5 (3-*C*H_2), 30.2, 30.3, 30.4, 30.5, 30.6, 30.7 (d) (2,4–8,10-*C*H_2), 37.64 (2′-*C*H_2CO), 39.8 (1-*C*H_2S), 40.4 (11-*C*H_2N), 62.2 (12′-*C*H_2OH), 68.3 (3′-*C*H_2O), 71.2, 71.3, 71.4, 71.6 (5′,6′,8′,9′-*C*H_2O), 73.6 (11′-*C*H_2O), 173.8 ppm (*C*ONH); MS (ES+): *m/z* (%): 407 (65) $[M+2H]^{2+}$, 418 (15) $[M+H+Na]^{2+}$, 814 (100) $[M+H]^+$, 836 (40) $[M+Na]^+$; HRMS: *m/z* calcd for $[M+H]^+$: 813.5327; found: 813.5328 ($\delta = 0.1$ ppm).

11-(12-amino-4,7,10-trioxadocecamido)undecyl-1-thio-(4-methoxytrityl) polystyrene resin: The azido acid **4** (79 mg, 319 μmol) was dissolved in CH_2Cl_2/DMF (1:1, 500 μL), DIPEA (166 μL, 959 μmol) was added and the resulting solution was cooled in an ice bath. TCFH (90 mg, 302 μmol) was added and the mixture gently swirled for 2 min before addition to the aminoundecyl resin **14** (200 mg, ≈160 μmol). This resin suspension was shaken for 65 h at RT, and the resin was filtered, washed with DMF, CH_2Cl_2, DMF, CH_2Cl_2, Et_2O (3 mL × 3 each solvent in order) and dried in vacuo to give a resin that returned a negative ninhydrin test result. This dried resin was resuspended in 1,4-dioxane/water (4:1, 2 mL), 1 M Me_3P in THF (960 μL, 960 μmol) was added and the mixture was gently swirled for 18 h. The solution was eluted and the resin rinsed with 1,4-dioxane, CH_2Cl_2, 1,4-dioxane, CH_2Cl_2 (3 mL × 3 each solvent in order). This resin was dried in vacuo and gave a strongly positive result to the ninhydrin test.

11-[12-(12-amino-4,7,10-trioxadocecamido)-4,7,10-trioxadocecamido]-undecyl-1-thio-(4-methoxytrityl) polystyrene resin (17): The coupling above was repeated (negative ninhydrin test), followed by the reduction step above (positive ninhydrin test) on the resin (≈160 μmol).

Di-1-{[12-(12-amino-4,7,10-trioxadocecamido)-4,7,10-trioxadocecamido]undecyl}disulfide diformate salt (2): The resin above (≈160 μmol) was treated with TFA and the residue oxidised using the same procedure as for **1** to yield a pale yellow oil. This oil was purified by RP-HPLC to give a white hygroscopic solid (116 mg, 60% based on the Fmoc quantification). HPLC (256 nm) 13.5 min; ^{1}H NMR (400 MHz, CD_3OD): $\delta =$ 1.30–1.50 (m, 32H; 3–10-CH_2), 1.72 (tt, $J = 7$, 7 Hz, 4H; 2-CH_2), 2.45–2.55 (m, 8H; 2′,2″-CH_2CO), 2.72 (t, $J = 7$ Hz, 4H; 1-CH_2S), 3.02 (br s, 2H; CON*H*), 3.14 (t, $J = 5$ Hz, 4H; 12′-CH_2N), 3.21 (t, $J = 7$ Hz, 4H; 11-CH_2N), 3.41 (t, $J = 6$ Hz, 4H; 12″-C$H_2NH_3^+$), 3.58 (t, $J = 6$ Hz, 4H; 11″-CH_2O), 3.61–3.85 ppm (m, 44H; 3′,5′,6′,8′,9′11′,3″,5″,6″,8″,9″-CH_2O); ^{13}C NMR (100 MHz, CD_3OD): $\delta = 28.9$ (9-*C*H_2), 30.3 (3-*C*H_2), 31.1, 31.2, 31.3, 31.4, 31.5, 31.6 (d) (2,4–8,10-*C*H_2), 38.3 (br), 38.5 (1,2′,2″-*C*H_2), 40.6 (12″-*C*$H_2NH_3^+$), 41.3 (11-*C*H_2N), 41.6 (12′-*C*H_2N), 69.1, 69.2 (3′,3″-*C*H_2O), 71.4 (11″-*C*H_2O), 72.1 (d), 72.2, 72.3, 72.4 (d) (5′,6′,8′,9′,10′,11′,5″,6″,8″,9″,10″-*C*H_2O), 171.2 (H*C*O_2^-), 174.6 (1′-*C*ONH), 174.9 ppm (1″-*C*ONH); MS (ES+): *m/z* (%): 609 (100) $[M+2H]^{2+}$, 1218 (50) $[M+H]^+$, 1240 (10) $[M+Na]^+$; HRMS: *m/z* calcd for $[M+H]^+$: 1217.7968; found: 1217.7940 ($\delta = 2.3$ ppm).

Preparation of SAMs of 1, 2 and 7: Gold (50 nm) was evaporated on to chromium-primed (2 nm) slides at a rate of 0.1–0.2 nms^{-1} at 10^{-7} bar. Slides and other glassware were cleaned using piranha solution, a 3:7 mix of 30% H_2O_2 and conc. H_2SO_4, before washing with copious amounts (6 rinses) of deionised water (18.2 MΩ) and drying in an oven overnight. *Caution: the preparation of piranha solution is highly exothermic and potentially violent in the presence of organic materials. Extreme care should be taken.* SAMs were formed by the incubation of gold-coated slides for a minimum of 18 h in 0.25 mM solutions of the appropriate disulfide in ethanol for **1**, or deionised water for **2**; or in 0.5 mM ethanolic solutions of **7**. The equilibrated SAMs were removed from solution, washed with HPLC grade ethanol, dried under a jet of N_2 and cut to size on a clean surface using a diamond scribe as needed.

SAM thiolate displacement by hexadecanethiol and XPS analysis: SAMs of **1**, **2**, and **7** were immersed in 10 mM solutions of hexadecanethiol in EtOH for a range of durations (4.5, 9, 18, 36, 48, 72 and 180 h). Samples were washed in HPLC grade ethanol (**1** and **7**) or nanopure water and then ethanol (**2**) then blow dried under an N_2 stream. Scans were collected at 20 keV and the C1s spectra for the different immersion durations were compared to virgin SAMs to determine rate of loss of ether carbons. Scans for each time point were taken for three different SAMs made on three different days. The ratio of the area of the C*C*O peak to the Au(4f) peak was therefore calculated for each sample.

SAM protein adsorption measurements by SPR analysis: Prior to each experiment, SAM chips were primed by flowing sample-matched aqueous biological buffer over them at 5 μLs^{-1} for a period of 30 min. For each type of protein and SAM chip, 5 μgml^{-1} protein solutions were injected into appropriately matched buffer carrier streams at a flow rate of 10 μLs^{-1} for a duration of 5 min. These were then followed with a buffer-only elution for 3 min, a 5 s injection of 0.1% w/v SDS and then buffer flow for a further minute.

Scanning near-field photolithography and protein array fabrication: Light from the frequency doubled argon ion laser was coupled to the end of the fiber probe through an optical coupler. Laser power of 4 mW was coupled to the NSOM fiber probe with an aperture size of 100 nm and a scan speed of 5 s per dot was used to generate the dot arrays and 0.2 μms^{-1} was used to create patterned lines. After patterning, the sam-

ples were dipped in a thiol/disulfide solution with contrasting terminal group (1 mM 16-hexadecanethiol, 1 mM 3-mercaptopropionic acid in EtOH) for at least 30 min to create the compositional chemical patterns. For patterns of **2**, a solution of 0.1 mM was used and the patterned chips were immersed for 18 h to give **18**. For the non-covalent immobilisation of proteins on patterned SAMs, the SNP-patterned SAM **18** was immersed in the IgG solution for 2.5 h, washed with PBS (5 times), water (once) and dried under an N_2 jet. For covalent immobilisation, SAM **18** was immersed in a 25% aq. solution of glutaraldehyde for 30 min, washed with water (5 times) and dried under an N_2 stream to give **19**. These SAMs were then exposed to IgG under the same conditions as above.

Acknowledgements

The authors wish to thank the EPSRC for funding through the "Snomipede" Basic Technology grant (EP/C523857/1) and a Life Science Interface fellowship (EP/F042590/1) for L.S.W. The donation of protein samples by Dr. Jenny Thirlway is also gratefully acknowledged.

[1] V. V. Tsukruk, *Adv. Mater.* **2001**, *13*, 95.
[2] B. A. Mantooth, P. S. Weiss, *Proc. IEEE* **2003**, *9*, 1785.
[3] N. L. Rosi, C. A. Mirkin, *Chem. Rev.* **2005**, *105*, 1547.
[4] R. J. Silbey, *Proc. Natl. Acad. Sci. USA* **2007**, *104*, 12595.
[5] A. M. Moore, B. A. Mantooth, Z. J. Donhauser, Y. Yao, J. M. Tour, P. S. Weiss, *J. Am. Chem. Soc.* **2007**, *129*, 10352.
[6] A. Ulman, *Chem. Rev.* **1996**, *96*, 1533.
[7] J. C. Love, L. A. Estroff, J. K. Kriebel, R. G. Nuzzo, G. M. Whitesides, *Chem. Rev.* **2005**, *105*, 1103.
[8] N. A. Amro, S. Xu, G.-Y. Liu, *Langmuir* **2000**, *16*, 3006.
[9] G.-Y. Liu, N. A. Amro, *Proc. Natl. Acad. Sci. USA* **2002**, *99*, 5165.
[10] S. Krämer, R. R. Fuierer, C. B. Gorman, *Chem. Rev.* **2003**, *103*, 4367.
[11] D. S. Ginger, H. Zhang, C. A. Mirkin, *Angew. Chem.* **2004**, *116*, 30; *Angew. Chem. Int. Ed.* **2004**, *43*, 30.
[12] X.-M. Li, J. Huskens, D. N. Reinhoudt, *J. Mater. Chem.* **2004**, *14*, 2954.
[13] B. D. Gates, Q. Xu, M. Stewart, D. Ryan, C. G. Willson, G. M. Whitesides, *Chem. Rev.* **2005**, *105*, 1171.
[14] G. J. Leggett, *Chem. Soc. Rev.* **2006**, *35*, 1150.
[15] C. Vieu, F. Carcenac, A. Pépin, Y. Chen, M. Mejias, A. Lebib, L. Manin-Ferlazzo, L. Couraud, H. Launois, *Appl. Surf. Sci.* **2000**, *164*, 111.
[16] W. Hu, K. Sarveswaran, M. Lieberman, G. H. Bernstein, *J. Vac. Sci. Technol. B* **2004**, *22*, 1711.
[17] R. D. Piner, J. Zhu, F. Xu, S. Hong, C. A. Mirkin, *Science* **1999**, *283*, 661.
[18] C. L. Cheung, J. A. Camarero, B. W. Woods, T. Lin, J. E. Johnson, J. J. De Yoreo, *J. Am. Chem. Soc.* **2003**, *125*, 6848.
[19] S. Sun, K. S. L. Chong, G. J. Leggett, *J. Am. Chem. Soc.* **2002**, *124*, 2414.
[20] M. Montague, R. E. Ducker, K. S. L. Chong, R. J. Manning, F. J. M. Rutten, M. C. Davies, G. J. Leggett, *Langmuir* **2007**, *23*, 7328.
[21] C. Bamdad, *Biophys. J.* **1998**, *75*, 1997.
[22] D. C. Chow, W.-K. Lee, S. Zauscher, A. Chilkoti, *J. Am. Chem. Soc.* **2005**, *127*, 14122.
[23] L. Wang, Q. Liu, R. M. Corn, A. E. Condon, L. M. Smith, *J. Am. Chem. Soc.* **2000**, *122*, 7435.
[24] C. D. Hodneland, Y.-S. Lee, D.-H. Min, M. Mrksich, *Proc. Natl. Acad. Sci. USA* **2002**, *99*, 5048.
[25] B. T. Houseman, J. H. Huh, S. J. Kron, M. Mrksich, *Nat. Biotechnol.* **2002**, *20*, 270.
[26] C. S. Chen, M. Mrksich, S. Huang, G. M. Whitesides, D. E. Ingber, *Science* **1997**, *276*, 1425.
[27] R. McBeath, D. M. Pirone, C. M. Nelson, K. Bhadriraju, C. S. Chen, *Dev. Cell* **2004**, *6*, 483.
[28] S. Sekula, J. Fuchs, S. Weg-Remers, P. Nagel, S. Schuppler, J. Fragala, N. Theilacker, M. Franzreb, C. Wingren, P. Ellmark, C. A. K. Borrebaeck, C. A. Mirkin, H. Fuchs, S. Lenhert, *Small* **2008**, *4*, 1785.
[29] J. C. Paulson, O. Blixt, B. E. Collins, *Nat. Chem. Biol.* **2006**, *2*, 238.
[30] R. L. Nicholson, M. Welch, M. Ladlow, D. R. Spring, *ACS Chem. Biol.* **2007**, *2*, 24.
[31] K.-Y. Tomizaki, K. Usui, H. Mihara, *ChemBioChem* **2005**, *6*, 782.
[32] G. J. Leggett, *Analyst* **2005**, *130*, 259.
[33] C. Wingren, C. A. K. Borrebaeck, *Drug Discovery Today* **2007**, *12*, 813.
[34] D. Witt, R. Klajn, P. Barski, B. A. Grzybowski, *Curr. Org. Chem.* **2004**, *8*, 1763.
[35] K. L. Prime, G. M. Whitesides, *Science* **1991**, *252*, 1164.
[36] C. Hoffmann, G. E. M. Tovar, *J. Colloid Interface Sci.* **2006**, *295*, 427.
[37] D. J. Vanderah, G. Valincius, C. W. Meuse, *Langmuir* **2002**, *18*, 4674.
[38] B. Merrifield, B. F. Gregg, *Methods Enzymol.* **1997**, *289*, 3.
[39] F. Zaragoza Dörwald, *Organic Synthesis on Solid Phase: Supports, Linkers, Reactions*, 1st. ed., Wiley-VCH, Weinheim, **2000**.
[40] P. Seneci, *Solid-Phase Synthesis and Combinatorial Technologies*, Wiley, New York, **2000**.
[41] R. Derda, D. J. Wherritt, L. L. Kiessling, *Langmuir* **2007**, *23*, 11164.
[42] E. Ostuni, R. G. Chapman, R. E. Holmlin, S. Takayama, G. M. Whitesides, *Langmuir* **2001**, *17*, 5605.
[43] S. Herrwerth, W. Eck, S. Reinhardt, M. Grunze, *J. Am. Chem. Soc.* **2003**, *125*, 9359.
[44] S.-W. Tam-Chang, H. A. Biebuyck, G. M. Whitesides, N. Jeon, R. G. Nuzzo, *Langmuir* **1995**, *11*, 4371.
[45] R. Valiokas, S. Svedhem, M. Ostblom, S. C. T. Svensson, B. Liedberg, *J. Phys. Chem. B* **2001**, *105*, 5459.
[46] O. Seitz, H. Kunz, *J. Org. Chem.* **1997**, *62*, 813.
[47] O. B. Wallace, D. M. Springer, *Tetrahedron Lett.* **1998**, *39*, 2693.
[48] S. Mourtas, C. Katakalou, A. Nicolettou, C. Tzavara, D. Gatos, K. Barlos, *Tetrahedron Lett.* **2003**, *44*, 179.
[49] M. Harre, K. Nickisch, U. Tilstam, *React. Funct. Polym.* **1999**, *41*, 111.
[50] J. T. Lundquist, J. C. Pelletier, *Org. Lett.* **2001**, *3*, 781.
[51] F. Debaene, N. Winssinger, *Org. Lett.* **2003**, *5*, 4445.
[52] C. Pale-Grosdemange, E. S. Simon, K. L. Prime, G. M. Whitesides, *J. Am. Chem. Soc.* **1991**, *113*, 12.
[53] Y. Li, N. M. Llewellyn, R. Giri, F. Huang, J. B. Spencer, *Chem. Biol.* **2005**, *12*, 665.
[54] L. S. Wong, J. L. Thirlway, J. Micklefield, *J. Am. Chem. Soc.* **2008**, *130*, 12456.
[55] L. S. Wong, F. Khan, J. Micklefield, *Chem. Rev.* **2009**, *109*, 4025.
[56] R. E. Ducker, S. Janusz, S. Sun, G. J. Leggett, *J. Am. Chem. Soc.* **2007**, *129*, 14842.
[57] N. P. Reynolds, S. Janusz, M. Escalante-Marun, J. Timney, R. E. Ducker, J. D. Olsen, C. Otto, V. Subramaniam, G. J. Leggett, C. N. Hunter, *J. Am. Chem. Soc.* **2007**, *129*, 14625.
[58] N. P. Reynolds, J. D. Tucker, P. A. Davison, J. A. Timney, C. N. Hunter, G. J. Leggett, *J. Am. Chem. Soc.* **2009**, *131*, 896.
[59] Y. Kobayashi, M. Sakai, A. Ueda, K. Maruyama, T. Saiki, K. Suzuki, *Anal. Sci.* **2008**, *24*, 571.
[60] S. Rauf, D. Zhou, C. Abell, D. Klenerman, D.-J. Kang, *Chem. Commun.* **2006**, 1721.
[61] H. Ihara, M. Takafuji, C. Hirayama, D. F. O'Brien, *Langmuir* **1992**, *8*, 1548.
[62] E. Kaiser, R. L. Colescott, C. D. Bossinger, P. I. Cook, *Anal. Biochem.* **1970**, *34*, 595.
[63] J. Eichler, M. Bienert, A. Stierandova, M. Lebl, *Pept. Res.* **1991**, *4*, 296.

Received: September 3, 2009
Revised: May 21, 2010
Published online: September 14, 2010

